Models and an efficient finite element scheme for the simulation of piezoelectric materials

M. Kaltenbacher[1], **B. Kaltenbacher**[2], **M. Nicolai**[3], **A. Schönecker**[3]
[1]*Applied Mechatronics, Alps-Adriatic University Klagenfurt, Austria*
e-mail: manfred.kaltenbacher@uni-klu.ac.at
[2]*Institute of Mathematics, Alps-Adriatic University Klagenfurt, Austria*
e-mail: barbara.kaltenbacher@uni-graz.at
[3]*Fraunhofer IKTS Dresden, Germany*
e-mail: Andreas.Schoenecker@ikts.fraunhofer.de

Abstract

Our models for piezoelectric materials are based on a decomposition of both dielectric displacement and mechanical strain into a reversible and an irreversible part. The reversible parts are described by the linear piezoelectric constitutive law. For the irreversible part we apply in our first model a phenomenological ansatz base on hysteresis operators and in the second one a micro-mechanical ansatz based on switching operations. For both models we achieve at similar extended constitutive laws, which we can uniformly treat within the partial differential equations and their numerical solution using the Finite Element (FE) method.

Keywords: finite element methods, ceramic, coupled fields

1. Introduction

Piezoelectric materials like lead zirconium titanate (PZT) are increasingly used in high power actuator applications. Modeling these actuators has presented a challenge to many researchers for quite some time. We present a phenomenological and a micro-mechanical based model and discuss their efficient numerical solution by applying the Finite Element (FE) method.

2. Mathematical Models

We follow the basic ideas discussed in [7] and decompose the physical quantities into a reversible and an irreversible part. For this purpose, we introduce the reversible part $\mathbf{D}^{\mathrm{r}}$ and the irreversible part $\mathbf{D}^{\mathrm{i}}$ (which is set equal to the irreversible polarization $\mathbf{P}^{\mathrm{i}}$) of the dielectric displacement as well as the reversible part $\mathbf{S}^{\mathrm{r}}$ and the irreversible part $\mathbf{S}^{\mathrm{i}}$ of the mechanical strain according to

$$\mathbf{D} \;=\; \mathbf{D}^{\mathrm{r}} + \mathbf{D}^{\mathrm{i}} = \mathbf{D}^{\mathrm{r}} + \mathbf{P}^{\mathrm{i}}\,; \quad \mathbf{S} = \mathbf{S}^{\mathrm{r}} + \mathbf{S}^{\mathrm{i}}\,. \tag{1}$$

The decomposition of the strain $\mathbf{S}$ is done in compliance with the theory of elastic-plastic solids under the assumption that the deformations are very small [1].

2.1. Phenomenological models using hysteresis operators

For this model approach, we compute the polarization from the history of the driving electric field $\mathbf{E}$ by a scalar hysteresis operator $\mathcal{H}$ [6]

$$\mathbf{P}^{\mathrm{i}} = \mathcal{H}[\mathbf{E}]\;\mathbf{e}_P\,, \tag{2}$$

with the unit vector of the polarization $\mathbf{e}_P$, set equal to the direction of the applied electric field. Taking this into consideration, we currently restrict our model to uni-axial loaded actuators. A more general approach, the multi-axial loading, would require a vector hysteresis operator. For the realization of $\mathcal{H}$ we use a scalar Preisach hysteresis operator. Therewith the output of the Preisach hysteresis operator then computes as [8]

$$\mathcal{H}[E](t) = \int_S \wp(\alpha,\beta)\gamma(\alpha,\beta)[E](t)\;\mathrm{d}\alpha\;\mathrm{d}\beta\,. \tag{3}$$

In (3) $\gamma(\alpha,\,\beta)$ defines the relay operator, $S = \{(\alpha\,,\beta) \in \mathbb{R}^2 \,|\, \beta \le \alpha\,\}$ the set of possible up and down switching thresholds and, and $\wp(\alpha,\beta)$ the Preisach weight function, which has to be identified from measurements [8].

The butterfly curve for the mechanical strain is modeled by a polynomial ansatz according to [6]

$$S^{\mathrm{i}} = \beta_1 \cdot \mathcal{H}[\mathbf{E}] + \beta_2 \cdot (\mathcal{H}[\mathbf{E}])^2 + ... + \beta_l \cdot (\mathcal{H}[\mathbf{E}])^l\,. \tag{4}$$

Similarly to [7] we define the tensor of the irreversible strains as follows

$$[\mathbf{S}^{\mathrm{i}}] = \tfrac{3}{2}\Big(\quad \beta_1 \cdot \mathcal{H}[\mathbf{E}] + \beta_2 \cdot (\mathcal{H}[\mathbf{E}])^2 + \cdots + \quad \beta_n \cdot (\mathcal{H}[\mathbf{E}])^n\Big)\,\Big(\mathbf{e}_P\,{\mathbf{e}_P}^T - \tfrac{1}{3}\,[\mathbf{I}]\Big)\,. \tag{5}$$

The parameters $\beta_1 \ldots \beta_n$ need to be fitted to measured data. Furthermore, the entries of the tensor of piezoelectric moduli are now assumed to be a function of the irreversible electric polarization $\mathbf{P}^{\mathrm{i}}$.

Finally, the constitutive relations for the electromechanical coupling can be established and written in d-form

$$\mathbf{S} \;=\; [\mathbf{s}^{\mathrm{E}}]\,\boldsymbol{\sigma} + [\mathbf{d}(\mathbf{P}^{\mathrm{i}})]^t\mathbf{E} + \mathbf{S}^{\mathrm{i}} \tag{6}$$

$$\mathbf{D} \;=\; [\mathbf{d}(\mathbf{P}^{\mathrm{i}})]\,\boldsymbol{\sigma} + [\boldsymbol{\varepsilon}^{\sigma}]\,\mathbf{E} + \mathbf{P}^{\mathrm{i}}\,. \tag{7}$$

2.2. Micro-mechanical Model

For the micro-mechanical model we consider the individual switching states and define the constitutive law as follows [3]

$$\begin{pmatrix} \mathbf{S} \\ \mathbf{D} \end{pmatrix} \;=\; \left(\sum_{I=1}^{M} \begin{pmatrix} [\mathbf{s}^{E}]_I & [\mathbf{d}]_I^t \\ [\mathbf{d}]_I & [\boldsymbol{\varepsilon}^{\sigma}]_I \end{pmatrix} \xi_I\right) \begin{pmatrix} \boldsymbol{\sigma} \\ \mathbf{E} \end{pmatrix} + \sum_{I=1}^{M} \begin{pmatrix} \mathbf{S}_I^{\mathrm{i}} \\ \mathbf{P}_I^{\mathrm{i}} \end{pmatrix} \xi_I\,. \tag{8}$$

In (8) M denotes the number of variants and ξ_I the volume fraction for variant I. The volume fractions compute by solving a system of ordinary differential equations, which couple the different switching states

$$\dot{\xi}_I = \sum_{J=1, J\neq I}^{K} \left(c_{JI}\xi_J^{\alpha} - c_{IJ}\xi_I^{\alpha} \right) . \tag{9}$$

The coefficients c_{IJ} compute by the transformation rates ω_{IJ}, which we define according to [2]

$$\omega_{IJ} = c_{IJ}\xi_I^{\alpha} = \omega_0 \, e^{-\frac{\Delta H(f_{IJ})}{kT}} \, \xi_I^{\alpha} \tag{10}$$

with the enthalpy of activation

$$\Delta H(f_{IJ}) = \Delta H_0 \left(1 - \frac{f_{IJ}}{f_*} \right) . \tag{11}$$

In (11) f_* denotes the driving force at which switching takes place and the actual driving forces f_{IJ} compute by

$$f_{IJ} = \mathbf{E} \cdot \Delta\mathbf{P}^{\mathrm{i}} + \boldsymbol{\sigma}^t \Delta\mathbf{S}^{\mathrm{i}} . \tag{12}$$

Here, $\Delta\mathbf{P}^{\mathrm{i}}$ and $\Delta\mathbf{S}^{\mathrm{i}}$ define the differences of the irreversible polarization as well as strain between two variants

$$\Delta\mathbf{P}^{\mathrm{i}} = \mathbf{P}^{\mathrm{i}}_J - \mathbf{P}^{\mathrm{i}}_I ; \quad \Delta\mathbf{S}^{\mathrm{i}} = \mathbf{S}^{\mathrm{i}}_J - \mathbf{S}^{\mathrm{i}}_I .$$

In the most commonly used ferroelectrics there exists a tetragonal phase with six distinct crystal variants and a rhombohedral phase with eight distinct crystal variants. In order to perform homogenization, we assume 14 distinct variants (see Fig. 1).

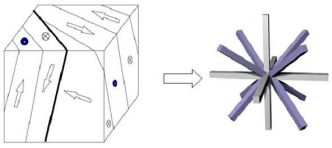

Figure 1: Homogenization of the distinct polarization states.

2.3. Partial Differential Equations

Studying the phenomenological (see (6), (7)) and the micro-mechanical approach (see (8), we can clearly see, that their structure is similar. Therefore, in the following we will only discuss the micro-mechanical approach. To do so, we will have to reformulate (8) in such a way, that the dependent physical quantities are the mechanical stress $\boldsymbol{\sigma}$ and electric displacement $\mathbf{D}$. Then using the governing equations for the mechanical and electrostatic fields (see , e.g., [4]) and incorporating our reformulated constitutive relation, results in

$$\rho\ddot{\mathbf{u}} - \mathcal{B}^t \left([\mathbf{c}^E]_{\mathrm{eff}} \mathcal{B}\mathbf{u} - \mathbf{S}^{\mathrm{i}} \right) - \mathcal{B}^t [\mathbf{e}]_{\mathrm{eff}} \tilde{\mathcal{B}}\varphi = 0 \tag{13}$$

$$\tilde{\mathcal{B}}[\mathbf{e}]_{\mathrm{eff}} \left(\mathcal{B}\mathbf{u} - \mathbf{S}^{\mathrm{i}} \right) - \tilde{\mathcal{B}} \cdot \left([\boldsymbol{\varepsilon}^S]_{\mathrm{eff}} \tilde{\mathcal{B}}\varphi - \mathbf{P}^{\mathrm{i}} \right) = 0 , \tag{14}$$

where the material tensors $[\,]_{\mathrm{eff}}$ are the effective tensors obtained by the sum over all variants weighted by the volume fractions, and $\mathcal{B}$, $\tilde{\mathcal{B}}$ are appropriate differential operators.

3. Finite-Element Scheme

A straight forward procedure to solve (13) and (14) is to put the hysteresis dependent terms (irreversible electric polarization and irreversible strain) to the right hand side and apply the FE method. Therewith, one arrives at a fixed-point method for the nonlinear system of equations. However, convergence can only be guaranteed if very small incremental steps are made within the nonlinear iteration process. A direct application of Newton's method is not possible, due to the lack of differentiability of the hysteresis operator. Therefore, we apply the so-called *incremental material parameter* method, which corresponds to a quasi Newton scheme applying a secant like linearization at each time step. For this purpose, we decompose the dielectric displacement $\mathbf{D}$ and the mechanical stress $\boldsymbol{\sigma}$ at time step t_{n+1} as follows

$$\mathbf{D}_{n+1} = \mathbf{D}_n + \Delta\mathbf{D}; \qquad \boldsymbol{\sigma}_{n+1} = \boldsymbol{\sigma}_n + \Delta\boldsymbol{\sigma} . \tag{15}$$

With this ansatz and some algebraic operations, we achieve the final system of PDEs for the increments of the mechanical displacement and scalar electric potential

$$\begin{aligned} &\mathcal{B}^t [\tilde{\mathbf{c}}^E_{n+1}] \mathcal{B}\Delta\mathbf{u} + \mathcal{B}^t [\tilde{\mathbf{e}}_{n+1}] \tilde{\mathcal{B}}\Delta\varphi = \\ &\qquad + \mathcal{B}^t [\tilde{\mathbf{c}}^E_{n+1}] [\Delta s^{\mathrm{E}}] \boldsymbol{\sigma}_n - \mathcal{B}^t [\tilde{\mathbf{c}}^E_{n+1}] [\Delta\mathbf{d}]^t \tilde{\mathcal{B}}\varphi_n \end{aligned} \tag{16}$$

$$\begin{aligned} &\tilde{\mathcal{B}}^t [\bar{\mathbf{e}}_{n+1}]^t \mathcal{B}\Delta\mathbf{u} - \tilde{\mathcal{B}} \cdot [\bar{\boldsymbol{\varepsilon}}^{\mathrm{S}}_{n+1}] \tilde{\mathcal{B}}\Delta\varphi = \\ &\qquad - \tilde{\mathcal{B}}^t \left([\Delta\mathbf{d}] - [\bar{\mathbf{d}}_{n+1}] [\tilde{\mathbf{c}}^{\mathrm{E}}_{n+1}] [\Delta\mathbf{s}^{\mathrm{E}}] \right) \boldsymbol{\sigma}_n \\ &\qquad - \tilde{\mathcal{B}}^t \left([\bar{\mathbf{d}}_{n+1}] [\tilde{\mathbf{c}}^{\mathrm{E}}_{n+1}] [\Delta\mathbf{d}]^t - [\Delta\boldsymbol{\varepsilon}^{\sigma}] \right) \tilde{\mathcal{B}}\varphi_n \end{aligned} \tag{17}$$

Applying a standard FE formulation, we obtain

$$\begin{aligned} &\begin{pmatrix} \mathbf{M}_{uu} & 0 \\ 0 & 0 \end{pmatrix} \begin{pmatrix} \Delta\underline{\ddot{\mathbf{u}}} \\ \Delta\underline{\ddot{\varphi}} \end{pmatrix} \\ &\quad + \begin{pmatrix} \mathbf{K}_{uu} & \tilde{\mathbf{K}}_{u\varphi} \\ \mathbf{K}_{\varphi u} & -\mathbf{K}_{\varphi\varphi} \end{pmatrix} \begin{pmatrix} \Delta\underline{\mathbf{u}} \\ \Delta\underline{\varphi} \end{pmatrix} = \begin{pmatrix} \underline{f}_u \\ \underline{f}_{\varphi} \end{pmatrix} . \end{aligned} \tag{18}$$

In (18) the vectors $\Delta\underline{\mathbf{u}}$ and $\Delta\underline{\varphi}$ contain all the unknown mechanical displacements and electric scalar potentials at the finite element nodes.

4. Implementation

The developed FE formulations, both with the phenomenological and with the micro-mechanical based models, have been implemented in CFS++ [5] and tested for practically relevant applications.

References

[1] E. Bassiouny and A. F. Ghaleb. Thermodynamical formulation for coupled electromechanical hysteresis effects: Combined electromechanical loading. *International Journal of Engineering Science*, 27(8):989–1000, 1989.

[2] A. Y. Belov and W. S. Kreher. Simulation of microstructure evolution in polycrystalline ferroelectrics ferroelastics. *Acta Materialia*, 54:3463 3469, 2006.

[3] J. E. Huber and N. A. Fleck. Multi-axial electrical switching of a ferroelectric: theory versus experiment. *Journal of the Mechanics and Physics of Solids*, 49:785 811, 2001.

[4] M. Kaltenbacher. *Numerical Simulation of Mechatronic Sensors and Actuators*. Springer, Berlin, 2. edition, 2007. ISBN: 978-3-540-71359-3.

[5] M. Kaltenbacher. Advanced Simulation Tool for the Design of Sensors and Actuators. In *Proceedings of Eurosensors XXIV*, Linz, Austria, September 5-8 2010. CD-ROM.

[6] M. Kaltenbacher, B. Kaltenbacher, T. Hegewald, and R. Lerch. Finite element formulation for ferroelectric hysteresis of piezoelectric materials. *Journal of Intelligent Material Systems and Structures*, 21:773–785, 2010.

[7] M. Kamlah and U. Böhle. Finite element analysis of piezoceramic components taking into account ferroelectric hysteresis behavior. *International Journal of Solids and Structures*, 38:605–633, 2001.

[8] I. D. Mayergoyz. *Mathematical Models of Hysteresis and Their Applications*. Elsevier, New York, 2003.